Pedro Alexandre Velez Fernandes

Licenciado em Ciências de Engenharia Eletrotécnica
e de Computadores

Capacity of a Massive MIMO-OFDM system using Millimetric Waves

Dissertação para obtenção do Grau de Mestre em
Engenharia Eletrotécnica e de Computadores

Orientador: Rui Dinis, Professor Associado com agregação, FCT-UNL

Co-orientador: Paulo Montezuma-Carvalho, Professor Auxiliar, FCT-UNL

Júri:

Presidente: Doutor João Pedro Abreu de Oliveira

Arguentes: Doutor Luís Filipe Lourenço Bernardo

Vogais: Doutor Paulo Miguel de Araújo B. M. de Carvalho

FACULDADE DE CIÊNCIAS E TECNOLOGIA
UNIVERSIDADE NOVA DE LISBOA

Setembro, 2016

Capacity of a Massive MIMO-OFDM system using Millimetric waves

Dedicated to my parents, my brother and sister….

Acknowledgement

My deepest gratitude to professor Rui Dinis and Paulo Montezuma-Carvalho for accepting me in this very interesting project and for always being there offering suggestions and guidance, without them this thesis would not have been completed. My special thanks to João Guerreiro, for his help, his advises, and for his great patience. Finally, I would like to give my heartfelt to my parents, brother and sister for their support and encouragement.

Abstract

In modern day society, wirelesses communications are fundamental to the communications worldwide. But with the saturation of the usable spectrum for communications, the need for capacity is one of the most important challenges faced nowadays.

With the development of technology, there is a much great need for quality of the service and bigger data streams. Increasing the capacity of a telecommunication system will allow to cope with that need.

The solution for the need for capacity, can be solved with the use of massive multiple input multiple output (MIMO) techniques, since MIMO system approach have already shown to increase the capacity of a wireless system.

The implications of this approach will make systems more complex and more energy consuming, in order to sustain the massive MIMO system. But such implementation combined with millimeter waves will allow the increase of the capacity of a system.

Keywords: Massive MIMO, Capacity Massive MIMO

Resumo

Na sociedade moderna, comunicações sem fios, são fundamentais para as comunicações a nível global. Mas com a saturação do espectro passível de ser utilizado, a necessidade por capacidade é um dos desafios mais importantes para os dias de hoje.

Com o desenvolvimento de tecnologia, existe cada vez mais uma necessidade de qualidade de serviço e de maior quantidade de dados. Aumentar a capacidade de um sistema de telecomunicações irá permitir cobrir essa necessidade.

A solução para a necessidade de capacidade, pode ser resolvida com o uso de técnicas massive input multiple output (Massive MIMO). Uma vez que a aproximação com sistemas MIMO, já demonstrou aumentar a capacidade de um sistema sem fios.

As implicações desta abordagem fará com que os sistemas tenham que se tornar mais complexos, e que consumam mais energia, de forma a conseguir suster o sistema massive MIMO. Porém tal implementação combinada com ondas milimétricas irá permitir o aumento da capacidade do sistema.

Palavras-chave: Massive MIMO, Capacidade Massive MIMO

Index of Contents

List of Figures

List of publications

This thesis consists of an overview and of the following publications which are referred to in the text by their Roman numerals.

I - P. Fernandes, J. Guerreiro, R. Dinis and P. Montezuma, “ On the Capacity of Nonlinear Massive MIMO-OFDM Systems ”, In Proc. of IEEE VTC'16 (Fall), Montreal, Canada, Sept. 2016

List of Abbreviations

5G - 5^{th} Generation

4G - 4^{th} Generation

3G - 3^{th} Generation

VLSI - Very-Large-Scale Integration

OFDMA - Orthogonal Frequency-Division Multiple Access

FDE - Frequency-Domain Equalization

MIMO - Multiple-Input Multiple-Output

ADSL - Asymmetric Digital Subscriber Line

SISO - Single-Input-Single-Output

ISI - Inter Symbol Interference

SNR - Signal-to-Noise Ratio

AWGN - Addictive White Gaussian Noise

NLOS - Non-Line-Of-Sight

PDF - Probability Density Function

BS - Base Stations

TDD - Time Division Duplexing

FDD - Frequency Division Duplexing

SISO - OFDM - Single Input Single Output Orthogonal Frequency-Division

IFFT - Inverse Fast Fourier Transformation

S/P - Serial to Parallel

P/S - Parallel to Serial

FFT - Fast Fourier Transformation

MRC - Maximal-Ratio Combining

LLR - Log-Likelihood Ratio

BPSK - Binary Phase-Shift Keying

STBC - Space Time Block Code

SSPA - Solid State Power Amplifier

DFT - Discrete Fourier Transform

1

1 - Introduction

Wireless systems are one of the most used and more important communication systems in the current days. In the past years, they have become the election choice for millions of users around the world, having democratize communications. Such development allowed the world to be more connected than ever, connecting the most remote zones of the world to the rest of the world. Massive MIMO have the capability of expanding even more its influence, if they can increase the quality and capacity. If such objectives are obtained the wireless systems will be able to become the most important communication system in use, substituting even optical fiber cable in some cases.

The 5^{th} generation(5G) are the proposed next generation telecommunication standards, that will substitute the present 4^{th} generation (4G) systems. 5G systems are being planned to allow greater capacity. With 5G systems, and therefore the increase in capacity, it will be possible to have more mobile broadband users per area, at the same time will allow the users to consume higher data quantities. That is possible thanks to the spectral efficiency, that 5G will allow. The use of 5G will also allow a better coverage and reduced latency.

1.1 - Overview of a Wireless system

Wireless communication systems have been a topic of study since 1960. The development of wireless communication technology is due to several reasons. First the demand by users for wireless connectivity increased in the past years. Second the development of Very-large-scale integration (VLSI) technology, enabled the implementation of small area circuits, low power signal processing and coding algorithms [1]. Third, the demand of high bit rates and high mobility increased in the last years with the advance of smartphones and PDA's or tablets.

In the 4G systems the spread spectrum radio technology used in 3G was abandoned and replaced with Orthogonal Frequency-Division Multiple Access (OFDMA) multicarrier transmission and other frequency-domain equalization (FDE) schemes, making possible to transfer very high bit rates despite multipath propagation effects and channel selectivity. The peak bit rate was further improved by smart antenna arrays for multiple-input multiple-output (MIMO) communications.

Wireless communication systems enabled the development of several applications, such as smart phones with Internet connection, industrial sensor networks, smart homes, wireless controlled cars, as several other applications in terms of autonomous health, security and leisure systems. The adaptability of the wireless systems as well as its reliability, allowed the expansion and development of new technology all across the globe, , at an accessible quality-price relation, democratizing the data and information access.

However, there are two significant technical challenges in supporting these applications: first is the phenomenon of fading due to time variation of the channel associated to small-scale effect of multi-path fading, as well as large-scale effect like the path loss by distance attenuation and shadowing by obstacles. Second, since wireless transmitter and receiver need to communicate over the air, there is significant interference between them.

Overall, the challenges are mostly because of limited availability of radio frequency spectrum and a complex time-varying wireless environment (fading and multipath). In nowadays, the key goal in wireless communication is to increase data rate and improve transmission reliability. In other words, the increasing demand for higher data rates implies better quality of service, fewer dropped calls, higher network capacity and user coverage calls. This can only be achieved by techniques that improve spectral efficiency and link reliability and more technologies in wireless communication were introduced, like OFDM and MIMO. [2]

1.2 – OFDM Multicarrier transmission

OFDM is a method of digital modulation in which the data stream is split into N parallel streams of reduced data rate, each of them transmitted on separate subcarriers. In short, it is a kind of multi-carrier digital communication method. OFDM has been around for about 40 years and it was first conceived in the 1960s and 1970s to minimize interference among channels near each other in frequency [3].

OFDM is employed in wireless and fixed communication systems standards such as asymmetric digital subscriber line (ADSL) broadband and digital audio and video broadcasts. OFDM is also successfully applied to a wide variety of wireless communication due to its high spectral efficiency and its robustness to multi-path delay [4].

In conclusion OFDM has been proposed as a transmission method to support high-speed data transmission over wireless links in multipath environments [5].

1.3- MIMO

MIMO has been developed for many years for wireless systems. One of the earliest MIMO implementations on wireless communications applications came in mid 1980 with the breakthrough developments by Jack Winters and Jack Saltz of Bell Laboratories [6]. They tried to send data from multiple users on the same frequency/time channel using multiple antennas both at the transmitter and receiver. After such experience several evolutions on the MIMO systems have been developed all across the world.

Now the interest in MIMO technology has aroused because when compared with Single-input-single-output (SISO) system, MIMO provides enhanced system performance under the same transmission conditions. First, a MIMO system greatly increases the channel capacity, which is proportional to the total number of transmitter and receiver arrays. Second, MIMO system provides the advantage of spatial diversity: each one transmitting signal is detected by the whole detector array, which not only improves system robustness and reliability, but also reduces the impact of inter symbol interference (ISI) and channel fading, since each signal determination is based on N detected results. In other words, spatial diversity offers N independent replicas of the transmitted signal. Third, the Array gain is also increased, which means a signal-to-noise ratio (SNR) gain achieved by focusing energy in desired direction [6]. The drawback of MIMO is the increased complexity in both the transmitter and receiver. With the use of Massive MIMO the problem escalates, since the implementation of massive MIMO is far more complex than the one used with MIMO, therefore it will require more energy in order to allow the system to work at is full potential.

1.4- Channel

In wireless communications there are several distortion effects and impairments in the communication channels. One cause is the multi-path effect, in which the signal will be reflected on several objects such as cars, buildings and others. Therefore the receiver antennas will receive the same signal several times, because the signal will follow several different paths and will arrive at different times (called time dispersion). Such effect creates multipath fading and intersymbolic interference. Fading due to multi-path spread is called frequency selective fading.

Other cause is the relative motion between receiver and transmitter which originates the Doppler effect as well as slow and fast fading.

A third cause is the signal attenuation, since the power received depends on the path length that the transmitted signal has to travel. When there is an obstacle between the transmitter and the receivers such as buildings, the most likely case to happen is the attenuation of the power of the signal. Finally, the noise that the system experiences, such as thermal noise in the receiver, atmospheric noise or noise resulting of the interference of wireless carriers, transmitters and systems. These types of noise are independent from the transmitted signals and from the channel. Such noises can be described as Addictive White Gaussian Noise (AWGN), although not all of types of noise can be described as AWGN.

1.4.1 – Multipath Effect

In conventional wireless systems such as SISO, where there is one transmitter antenna and one receiver antenna, multipath effect can occur. Such effect can be described as the signal being reflect in inanimate objects creating several replicas of the original signal. The several replicas will be perceived at the receptor with different phases, amplitudes and angles.

In figure 1.1 it can be seen the representation of the multipath effect, where the signal is reflected on buildings, the different colors serve as a demonstration of the alterations that the signal is submitted, when it is reflected.

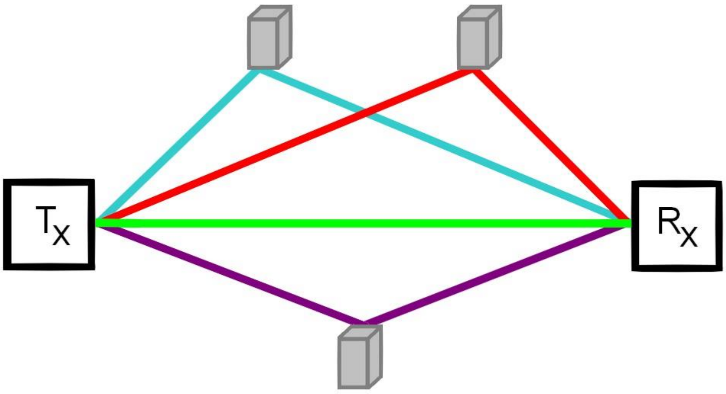

Fig 1.1- Multipath effect

The multipath effect may cause several interferences, creating an increase in number of errors, lowering the quality of the signal and therefore a reduction in data speed.

Regarding the fading we can have two different: flat fading and frequency selective fading. When the transmission occurs, the signal can be affected on its amplitude and phase. If the transmitted signal experiences an alteration in all of its spectral components with the same amplitude gains and phase shifts, the channel is called flat fading channel. Frequency selective fading will induce intersymbol interference, which can be compensated by digital processing. Assuming a single transmitted impulse, whose time duration T_m is the duration between the first and last received component that possesses the maximum delay spread, therefore the coherence bandwidth f_c is $\frac{1}{T_m}$. As we all know, symbol time is T_s. A channel is said to frequency selective fading if T_m>T_s and it is said to suffer flat fading if T_m<T_s . [7]. In this particular case, the transmitted signal bandwidth is much smaller than the channel's coherent bandwidth. Flat fading channel occurs in many wireless environments and causes deep fades. The amplitude distribution of flat fading is either Raleigh distribution or Ricean distribution.

1.4.3 – Rayleigh Fading

The Rayleigh distribution is used to model the multipath fading effect, in a case where non-line-of-sight (NLOS) transmission occurs, which means that the signal perceived at the receiver is the result of the reflections. In this case, the probability density function (PDF) of fading amplitude of the i^{th} path a_i is given by

$$f_{\alpha_i}(\alpha_i) = \frac{2\alpha_i}{\Omega_i} exp\left(-\frac{\alpha_i^2}{\Omega_i}\right), \alpha_i \geq 0, \quad (1.1)$$

where Ω_i= E [a_i^2] and exp[·]denotes the expectation of its argument [8].

In the case where it exists line of sight, the Rician fading is more applicable.

1.4.4 – Doppler Fading

In wireless communications where there is relative movement of the elements of the system i.e. the receiver moves away or closer to the transmitter, the Doppler effect (shift) may occur. The Doppler effect is the change in frequency/wavelength due to relative motion to the source of the waves. The Doppler effect is directly proportional to the magnitude of the relative speed and is modeled here as a contribution to the carrier frequency. For waves which do not require a medium, only the relative difference in velocity between the observer and the source needs to be considered [9]. In figure 1.2 it is possible to see the representation of the Doppler effect, showing the effect that the movement of the receptor to the transmitter has on the frequency of the transmitted wave. It is possible to observe the stationary case, the case where the receiver is moving away from the transmission source and the case where the receiver is moving towards the transmission source.

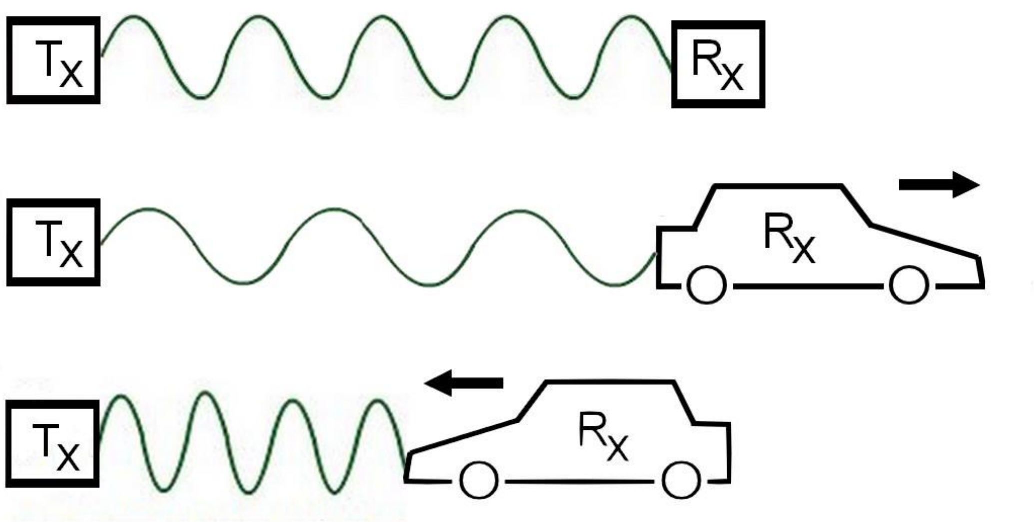

Fig. 1.2 - Doppler effect

Because the detected frequency increases as the receiver is moving toward the observer, the source's velocity must be subtracted when motion is moving toward the observer. Therefore when receiver is moving away from the observer the detected frequency decreases, so the source’s velocity must be added when the motion is moving away from the observer.

The phase difference between two transmission paths is given by

$$\Delta\phi = \frac{2\pi\Delta l}{\lambda} = \frac{2\pi\Delta t}{\lambda}\cos\theta. \quad (1.2)$$

The Doppler shift is given by

$$f_d = \frac{1}{2\pi}\cdot\frac{\Delta\phi}{\Delta t} = \frac{v}{\lambda}\cos\theta. \quad (1.3)$$

If a pure sinusoid wave is transmitted, a range of frequencies adjacent to this sinusoid frequency will be received. The Doppler shift broadens the spectrum of the received signal by spreading the basic spectrum in frequency domain. If the signal spectrum is wide enough compared to this spreading, the effect is not noticeable, otherwise, distortion will occur.

Both multi-path fading and Doppler effects can impair the reception of the transmitted signal. It is also well known that ISI happens when multiple paths are received with various delays and co-channel users create distortion to the target user. And thermal noise is electronic white noise that definitely needs to be counted in. Diversity, as stated by Proakis [10] is an effective way to improve error rate performance in fading channels. MIMO OFDM is introduced as a scheme in wireless communications to offer diversity, capacity and array gain [11]

1.4.5 – Slow and fast Fading

The Doppler effect fading effect creates a spread, that can be divided in Fast Fading and slow fading. In wireless communication, a channel can be time varying and those dynamic channels are characterized as slow or fast fading channels. Fast fading channel changes significantly during the duration of a symbol. And when the channel varies rapidly, it distorts the symbol's amplitude and phase erratically over its interval. On the other hand, slow fading occurs when the channel changes much slower than one symbol duration. This does not imply that the effects of the channel can be neglected, but it is possible to track the changes in the channel to appropriately compensate for channel dynamics. We define coherence time T_c of the channel as the period of time over which the fading process is correlated. T_c is closely related to Doppler spread f_d as:

$$T_c = \frac{1}{f_d}. \quad (1.4)$$

If the symbol time duration T_s is smaller than T_c, the fading is slow fading, otherwise, the channel fading is considered fast fading [12].

1.5 – Overview of Massive MIMO

Since MIMO gains increase with the number of antennas, there is interest in MIMO systems with a huge number of antennas, usually denoted massive MIMO schemes. Massive MIMO schemes where a given base stations (BS) with several tens or even hundreds of antenna elements communicates simultaneously with several tens of MTs are being proposed for 5G systems [13].

Although the potential capacity gains can be very high, the implementation complexity of MIMO schemes grows very fast with the number of antenna elements. Therefore, massive MIMO schemes cannot be regarded as a scaled version of conventional MIMO schemes, and low-complexity implementations are required [14].

In massive MIMO the number of transmitters is large, so a time division duplexing (TDD) is preferable in opposing to a frequency division duplexing (FDD), because that with TDD adding more antennas does not affect the resources needed for the channel estimation. Because of the large number of BS antennas and the number of users are large, the signal processing at the terminal end must deal with large dimensional matrices/vectors. Thus, simple signal processing is preferable. In Massive MIMO, linear processing (linear combining schemes in the uplink and linear precoding schemes in the downlink) is nearly optimal.

Massive MIMO is scalable. The BS learns the channels via uplink training, under TDD operation. The time required for channel estimation is independent of the number of BS antennas. Therefore, the number of BS antennas can be made as large as desired with no increase in the channel estimation overhead. Furthermore, the signal processing at each user is very simple and does not depend on other users' existence, i.e., no multiplexing or de-multiplexing signal processing is performed at the users. Adding or dropping some users from service does not affect other users activities.[15]

1.6 Channel Capacity

Capacity of systems has been widely studied across the years. The channel capacity is defined as the tight upper bound on the rate at which information can be reliably transmitted over a communication channel. For a linear single input single output Orthogonal Frequency-Division (SISO- OFDM) transmission in ideal additive white Gaussian noise AWGN channels, the capacity is [16]

$$C = B\log_2(1 + SNR). \qquad (1.5)$$

By the Shannon Hartley theorem, where C represents the capacity, B the bandwidth and SNR represents the signal to noise ratio that is $\frac{S}{N}$. The representation of the SISO system being considered for this results can be seen in Fig 1.3

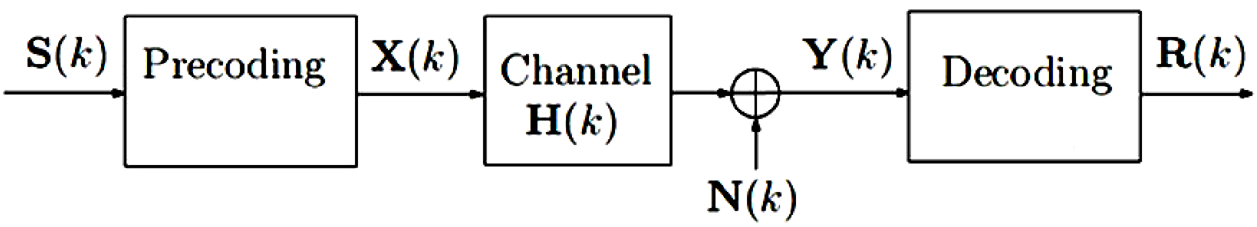

Fig 1.3 – SISO system

This model will serve as the base for the study of the capacity of massive MIMO with linear and non-linear effects. Since that after the precoding and decoding operation, such approach is valid to the analysis of the capacity of Massive MIMO.

2

2-Existing techniques

In this chapter it will be presented the existing communication techniques used to deal with the MIMO transmission. First it will be presented the OFDM used to improve the results of the channel. Second the MIMO systems architecture. Third it will be presented the MIMO-OFDM system that combines a MIMO system with the OFDM technique. We then will explore the diversity combining techniques and beamforming. Finally, we will characterize the user separation techniques used to deal with the effects of the channel.

2.1 – OFDM techniques

In OFDM, a block of data is converted into a parallel form and mapped into each subcarrier in the time domain. By transmitting the symbols in parallel, the interval between the signals becomes much larger and this effectively eliminates ISI in time dispersive channels. Inverse fast Fourier transformation (IFFT) is used to transfer the signal from time domain to frequency domain. It takes N symbols at one time where N is the number of subcarriers in the system. Each of these N input symbols has a period of T seconds. As we know, the basic functions for an IFFT are N orthogonal sinusoids. Each input symbol acts like a complex weight for the corresponding sinusoidal basis function. Since the input symbols are complex, the value of the symbol determines both the amplitude and phase of the sinusoid for that subcarrier. The IFFT output is the sum of all N sinusoids. Thus, the IFFT block provides a simple way to modulate data onto N orthogonal subcarriers. The block of N output samples from the IFFT makes up a single OFDM symbol [17].

In the Fig 2.1 we can see the basic structure of an OFDM transmitter.

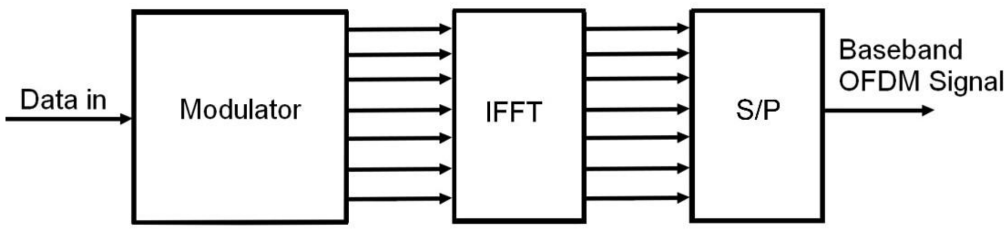

Fig 2.1 – Basic OFDM transmitter.

The signal is then submitted to a serial to parallel conversion (S/P), where the serial bitstream is converted into several parallel bitstreams to be divided among the individual carriers. After that the signal is transmitted through the channel, being the channel the route that the signal goes through from the receiver to the transmitter. When the frequency signals reach the receiver, the receiver must perform the synchronization (both in time and frequency), channel Estimation, demodulation and decoding. At the receiver the data processing is converted using a parallel to serial conversion (P/S) and a fast Fourier transformation (FFT) block is firstly used to transfer the received time-domain signal into frequency-domain. Ideally, the output of the FFT block should be identical to the transmitted symbols before the IFFT block. Assuming that the information about the channel is know, the symbols will be demodulated and estimated based on this channel information.

In Fig 2.2 we can see the basic structure of a OFDM receiver.

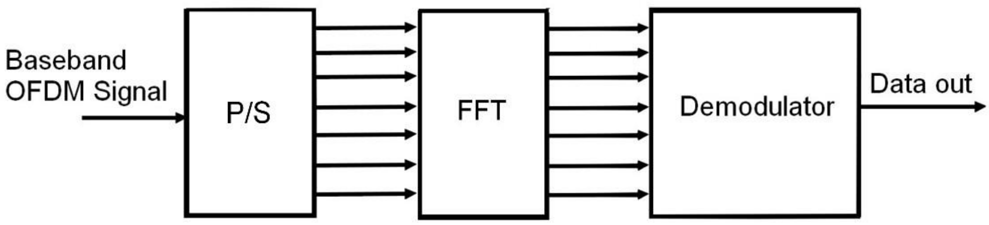

Fig 2.2 – Basic OFDM Receiver.

When there is more than one transmission path between the transmitter and the receiver, or the received signal is the sum of many versions of the transmitted signal with different delays and attenuations, it causes ISI effect. To reduce this effect, two methods are generally used in the OFDM scheme: parallel data transmission and cyclic prefix. Usually the length of the cyclic prefix is longer than the length of the channel's impulse response. The basic idea is to replicate part of the OFDM time-domain block from the back to the front to create a guard period. The duration of the guard period T_g should be longer than the worst-case delay spread of the channel. The structure of cyclic prefix is illustrated in Figure 2.3, [18].

Fig 2.3 – Signal with Cyclic prefix

OFDM signals are known to have substantial envelope fluctuations, which lead to amplification difficulties. Such problem can be aggravated in MIMO-

OFDM schemes [19]. In the last years, several techniques to combat the large envelope fluctuations of OFDM signals have been proposed [20]. The simplest ones based on nonlinear clipping operations [21], [22].

2.2 – MIMO System

MIMO is a technology that uses multiple antennas at the transmitter and at the receiver to transmit and receive signals. In the Fig. 2.4 it is shown the basic concept of a MIMO system.

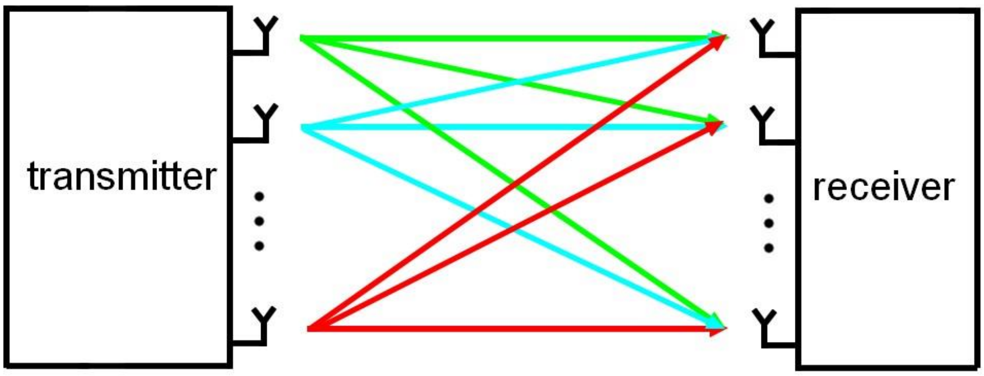

Fig 2.4 – MIMO structure.

In a MIMO system, the data $[x_1, x_2, \ldots . x_N]$ is transmitted with N transmitting antenna arrays. The receiver is composed by M (M≥N) antenna arrays. Let r_j(j= 1, 2,..., M) represents the signal received by the j^{th} antenna. The signals received at the receiver can be represented as:

$$r_1 = h_{11}\, x_1 + h_{12} x_2 + \cdots + h_{1N} x_N\,, \quad (2.1)$$

$$r_2 = h_{21}\, x_1 + h_{22} x_2 + \cdots + h_{2N} x_N\,, \quad (2.2)$$

$$r_M = h_{M1}\, x_1 + h_{M2} x_2 + \cdots + h_{MN} x_N, \qquad (2.3)$$

where h ij is a weight coefficient that represents the impact of the j^{th} transmitting signal x_j on the j^{th} receiver signal strength. We define a frequency channel matrix H as:

$$H=\begin{pmatrix} h_{11} & h_{12} & \cdots & h_{1N} \\ h_{21} & h_{22} & & h_{2N} \\ \vdots & \vdots & \ddots & \vdots \\ h_{M1} & \mathrm{h}_{\mathrm{M2}} & \cdots & h_{MN} \end{pmatrix}. \quad (2.4)$$

Therefore, in MIMO system, the transmitted signals $\{x_i\}$ can be recovered by estimating the channel matrix H and the receiving signal vector R.

MIMO systems can provide two types of gains: diversity gain and spatial multiplexing gain. It is known that there is a fundamental tradeoff between these two gains: higher spatial multiplexing gain comes at the price of sacrificing diversity [23]. Diversity is used in MIMO to combat channel fading. Since in MIMO each pair of transmitting and receiving antennas provides a signal path from the transmitter to the receiver and each path carries the same information simultaneously, the signal achieved in the receive antenna is more reliable and the fading can be effectively decreased. If the path gains between individual transmit–receive antenna pairs fade independently, in this case multiple parallel spatial channels are created. By transmitting independent information streams in parallel through the spatial channels, the data rate can be increased. This effect is also called spatial multiplexing [24].

The benefit of using diversity is a higher SNR and a lower error probability and the benefit of using multiplexing is that it allows a higher rate. Diversity requires that the same information is sent by all the antennas, and multiplexing requires independent information to be sent by each antenna. Because of that particularity, it is required that there is a selection of each one should be used, in order to get the benefits required from the use of one or the other accordingly to the location requirements.

2.3 – MIMO-OFDM System

MIMO OFDM is a technology that combines MIMO and OFDM together to transmit data in wireless communications in order to deal with frequency selective channel effect. The OFDM signal on each subcarrier can overcome narrowband fading, therefore, OFDM can transform frequency-selective fading channels into parallel flat ones. Then by combining MIMO and OFDM technology together, MIMO algorithms can be applied in broadband transmission [25].

A MIMO OFDM system transmits data modulated by OFDM from multiple antennas simultaneously. At the receiver, after OFDM demodulation, the signal is recovered by decoding each one of the sub-channels from all the transmit antennas [26]. MIMO-OFDM takes advantage of the multipath properties of environments using base station antennas without NLOS. By using MIMO and OFDM, a higher throughput can be achieved.

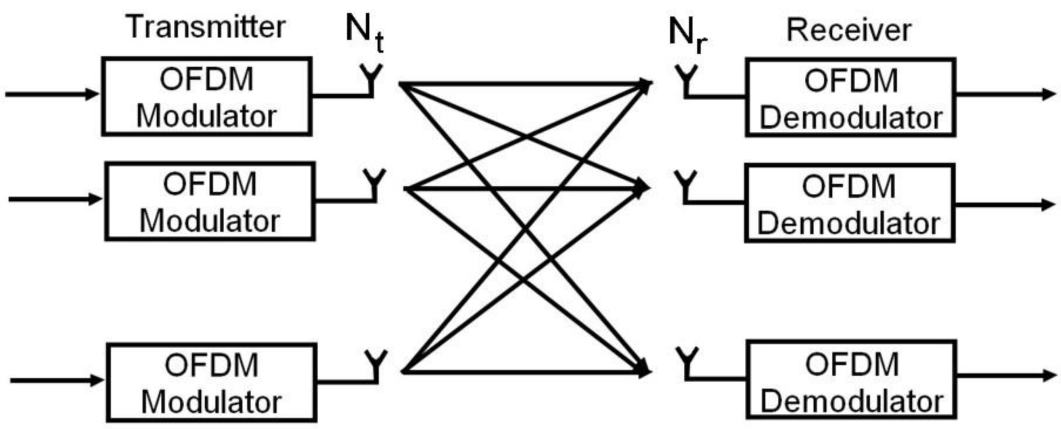

Fig 2.5- Basic structure MIMO-OFDM

In Figure 2.5, the basic structure of MIMO OFDM is shown. In this figure, the signals are modulated by a OFDM modulator, then they are transmitted by

MIMO system, finally, the signals are recovered by the OFDM demodulator. Therefore, MIMO OFDM achieves spectral efficiency, increased throughput and ISI can thus be prevented.

2.4 – Diversity combining techniques

Nowadays, the most popular transmit diversity techniques in use are Selection diversity, space time coding (Alamouti scheme) and beamforming techniques. It will be also explored the usage of Maximal-Ratio combining (MRC) in which the estimations of different channels are coherently combined to recover the transmit signals.

2.4.1 – Selection Diversity

In MIMO systems, selection diversity selects the branch providing the largest magnitude of log-likelihood ratio (LLR). The LLR for Binary Phase-shift keying (BPSK) signals in fading channels is found to be proportional to the product of the fading amplitude and the matched filter output after phase compensation.

Channel state includes statistics information such as fading amplitudes, phases and delay. In selection diversity technique, none of these channel information parameters are required. Selection diversity uses one receiver antenna which greatly reduces the complexity of the wireless systems. Here, the receiver simply looks at the outputs from each fading channel and selects the one with the highest SNR. In this case, the strongest signal is picked up and other signals that have undergone deep fades are unlikely to be picked by the receiver, which can avoid the deep fading effect. Therefore, the more the channels are, the more accurate the recovered signal would be. There is also no need for any addition of the fading channel outputs, which further decreases the complexity. Since Selection diversity does not require any knowledge of the phases, it is usually used in non-coherent or differential coherent modulation schemes. The signals from the transmitter antenna are sent through multiple channels, selected by the detector system and finally received by the receive antenna. The structure for this type of diversity can be seen in Fig. 2.6

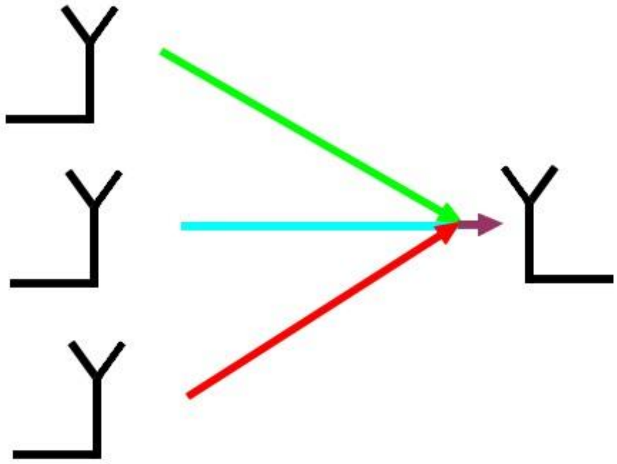

Fig.2.6 – Basic structure of transmit selection diversity.

2.4.2 – Alamouti Scheme

Alamouti scheme is an orthogonal transformation scheme that gives the second order transmission diversity, which is applied to the receiver that can greatly reduce the complexity of the receiver. The Alamouti scheme also assumes that the channel is invariant in the two transmission intervals.

2.4.3 – Alamouti Scheme with two transmitter antennas one receiver antenna

The MIMO Alamouti code is a simple space time block code (STBC), where the different replicas sent for exploiting diversity are generated by a space-time encoder which encodes a single stream through space using all the transmit antennas and through time by sending each symbol at different times.

The Alamouti STBC scheme uses two transmit antennas and Nr receive antennas and can accomplish a maximum diversity order of 2Nr.

At the transmitter of the Alamouti scheme, the two signals x_1 , x_2 are transmitted at the same time from the two transmitting antennas. In this case, x_1, x_2 are baseband complex symbols carrying the information.

The time and transmit sequence are shown as the following:

Time	Antenna1	Antenna2
T	X_1	X_2
t+T	-X_2 *	X_1 *

Symbols x 1 and x 2 are sent with the first beam at time t, while -X_2 *and X_1* (* stands for complex conjugate) are transmitted through the second antenna at time t+T, where T is the symbol duration[27]. Where we assume that the rows of each coding scheme represent a different time instant, while in this case, the first and second rows represent the transmission at the first and second time instant respectively.

The channel model is

$$h_1 = h_{1(t+T)} = H_1 = a_1 e^{j\theta_1} \qquad (2.7)$$

$$h_2 = h_{2(t+T)} = H_2 = a_2 e^{j\theta_2}$$

At the receiver of the Alamouti scheme, the signals are respectively received at times t and t+T, where

$$R_1 = H_1 X_1 + H_2 X_2 + N_1 \qquad (2.8)$$

$$R_2 = -H_1 X_2^* + H_2 X_1^* + N_2$$

Here r_1, r_2 are the received signals and n_1 , n_2 are the complex random variables representing the noise and interference. The received symbols are then combined and processed by the decoder. The receivers obtain the signals s_1 , s_2 through the following matrix after computing the estimates of the complex channel gains, that is,

$$S_1 = H_1^* R_1 + H_2 R_2^* \qquad (2.9)$$

$$S_2 = H_2^* R_1 - H_1 R_2^*$$

2.4.4 – Alamouti Scheme two transmitter antennas two receiver antenna

When it is used an Alamouti scheme with two transmitter antennas and one receiver antenna its possible to have a diversity of 2. When a Alamouti scheme with two transmitter antennas and two receiver antennas is used, it is possible to have a diversity of 4. In this case, the transmission sequence has minor change from the two transmitters and one receiver Alamouti scheme [28].

The transmitting signals at the transmitting antennas are the following:

Time	Antenna1	Antenna2
T	X_1	X_2
t+T	-X_2*	X_1 *

where symbols $X_1$and X_2 are sent with the first beam at time t, while -X_2 *and X_1* are transmitted through the second beam at time t+T, where T is the symbol duration.

The receiving signals at the receiving antennas are shown in the following format:

Time	Antenna1	Antenna2
T	R_1	R_2
t+T	R_3	R_4

There are four communication channels between the two transmitter antennas and two receiver antennas, which are defined as $H_1, H_2. H_3, H_4$ respectively. The relationship between the receiving and transmitting signals can be represented as:

$$R_1 = H_1X_1 + H_2X_2 + N_1$$

$$R_2 = -H_1X_2^* + H_2X_1^* + N_2 \qquad (2.10)$$

$$R_3 = H_3X_1 + H_4X_2 + N_3$$

$$R_4 = -H_3X_2^* + H_4X_1^* + N_4,$$

where X_1, X_2 represent the transmitted signals R, R_2, R_3, R_4 are the received signals and N_1, N_2, N_3, N_4 are complex random variables representing the noise and interference. The receivers then obtain the signals S_1, S_2 after computing the estimates of the complex channel gains, that is,

$$S_1 = H_1^*R_1 + H_2R_2^* + H_3^*R_3 + H_4R_4\,, \qquad (2.11)$$

$$S_2 = H_2^*R_1 - H_1R_2^* + H_4^*R_3 - H_3R_4^*\,.$$

In this case, the results of this scheme are equivalent to those obtained by the 4-branch MRC scheme [29].

2.4.5 – Beamforming technique

In beamforming transmission scheme, usually the CSI should be known at the transmitter, so we use the known channel information to code the transmitting signals. Then at the receiver side, the equalization process is greatly simplified. For example, in a one-transmitter–two-receiver Beamforming scheme, assume that the transmitted signal is X, the first channel as H_1 and the second channel as H_2 where

$$H_1 = a_1 e^{j\theta 1} \qquad (2.12)$$

$$H_2 = a_2 e^{j\theta 2}.$$

The signal transmitted by the first transmitting antenna is XH_1^* and the signal transmitted by the second transmitting antenna is, XH_2^*.

After going through the channels, signals that are received by the receivers could be represented as:

$$R_1 = X\, H_1^* H_1 + N_1 = a_1^2 x + N_1, \qquad (2.13)$$

$$R_2 = X\, H_2^* H_2 + N_2 = a_2^2 x + N_2,$$

where $R_{1,}$, R_2 are the received signals and N_1, N_2, are complex random variables representing the noise and interference.

The combining scheme for two-branch Beamforming is:

$$S' = R_1 + R_2 = a_1^2 x + N_1 + a_2^2 X + N_2 \qquad (2.14)$$

$$= (a_1^2 + a_2^2)x + N_1 + N_2.$$

After equalizing the coefficient $(a_1^2 + a_2^2)$, we can get the final signal after decision making. The benefits of MIMO beamforming is that the power gain and array gain get increased and the co-channel inter-cell interference is reduced. Also the diversity gain get increased, because Beamforming can combat the fading effects of the channel.

2.4.6 – Maximal-ratio combining (MRC)

The MRC is a diversity technique over fading channels. While it is slightly more complex than Selection Diversity, the performance is especially good in the case of independent fading channels.

MRC selects all the branches and gets the average square value of each branch to decrease Rayleigh fading. The basic structure of MRC scheme is illustrated in Figure 2.7.

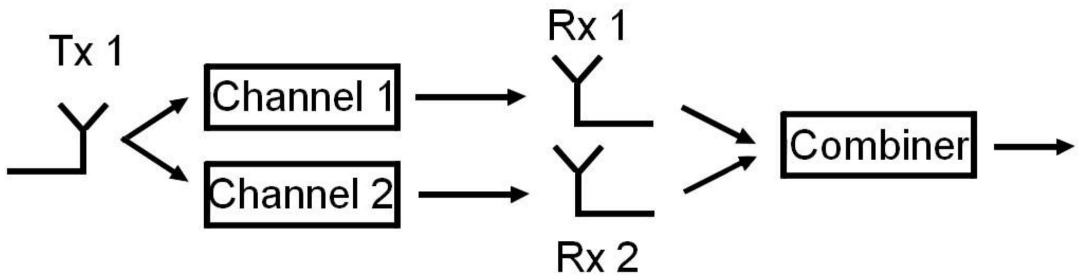

Fig 2.7 Basic structure of Maximal-ratio Receiver Combining.

Let us first consider a one-transmitter-two-receiver MRC model. At a given time, a signal x is sent from the transmitter. The channels between the transmit antenna and the receive antennas are denoted by H_1 and H_2 given by

$$H_1 = a_1 e^{j\theta 1}, \quad (2.15)$$

$$H_2 = a_2 e^{j\theta 2}.$$

Considering the noise and interference added at the two receivers, the resulting received signals could be written as:

$$R_1 = H_1 X + N_1, \quad (2.16)$$

$$R_1 = H_2 X + N_2,$$

where $R_{1,} R_2$ are the received signals and $N_{1,} N_2$ are complex random variables representing the noise and interference.

After the combiner we have:

$$S' = H_1^* R_1 + H_2^* R_2 = H_1^* (H_1 X + N_1) + H_2^* (H_2 X + N_2) \qquad (2.17)$$

$$= (a_1^2 + a_2^2) X + H_1^* N_1 + H_2^* N_2.$$

Then after equalizing the coefficient $a_1^2 + a_2^2$, we can get the final signal after decision making.

3

Capacity of the System

In this chapter we describe the results of capacity for several systems, that were the result of a developed software program, that simulates the SISO and MIMO system. First we describe the capacity for a linear SISO system. Second the capacity for a nonlinear SISO system. Third the capacity for a linear MIMO system, and finally the capacity for a nonlinear MIMO system. The channel is frequency-selective and based on a cluster ray model where the antennas have a correlation factor. In the case of MIMO-OFDM it will be considered a scenario with T transmitter antennas and R receiver antennas. The total number of multi-path components is L = G X B, where G is the number of clusters of B rays. The channel is represented by the R X T matrix given by

$$h(t) = \sum_{l=0}^{L-1} \boldsymbol{\beta}^{(l)} \delta(t - \tau_l) \ , \qquad (3.1)$$

where τ_l and $\beta^{(l)}$ are the delay and the channel matrix associated with the l^{th} tap. The channel matrix for the l^{th} path is,

$$\beta^{(l)} = \begin{bmatrix} \beta_{1,1}^{(l)} & \beta_{1,2}^{(l)} & \cdots & \beta_{1,t}^{(l)} \\ \beta_{2,1}^{(l)} & \beta_{2,2}^{(l)} & \cdots & \beta_{2,t}^{(l)} \\ \vdots & \cdots & \ddots & \vdots \\ \beta_{r,1}^{(l)} & \cdots & \cdots & \beta_{r,t}^{(l)} \end{bmatrix}, \tag{3.2}$$

where $\beta_{r,t}^{(l)}$ is the fading coefficient between the r^{th}receive antenna and the t^{th} transmit antenna for the l^{th} tap. Each OFDM block is formed by P = min(T; R) streams with N_t subcarriers and is represented by the $P\ X\ N_t$ matrix

$$S = \begin{bmatrix} S^{(0)} \\ S^{(1)} \\ \vdots \\ S^{(P)} \end{bmatrix} = [S(0) \quad S(1) \quad \cdots \quad S(p)]. \tag{3.3}$$

This matrix can be decomposed along its lines or its columns. On one hand, we use the $1\ x\ N_T$ matrix $S^{(p)} = \begin{bmatrix} S_1^{(p)} & S_2^{(p)} & \cdots & S_{NT}^{P} \end{bmatrix}$ to represent the set of data symbols associated to the p^{th} stream. On the other hand, we use the P x 1 matrix $S = [S(k)_1 \quad S(k)_2 \quad \cdots \quad S(k)_p]^T$ to define the set of data symbols associated to the k^{th} subcarrier. Regarding the composition of each OFDM signal, only N of the N_T subcarriers are effectively used to transmit data. The other N_G = N(M-1) subcarriers are left idle so as to obtain an oversampling operation by a factor of M. Therefore, $S(k)_p = \pm\sigma_S \pm j\sigma_S$ and $E[|S(k)_p|^2]$= $2\sigma\sigma_S^2$ for k ∈ N and $S(k)_p =$ 0.

The signal will then be submitted to a precoding technique. It will be considered the SVD technique for the precoding and decoding operation because of its properties, and because we are interested in the system capacity [29][30]. Of course, such precoding and decoding operation requires the perfect channel knowledge at the receiver and transmitter.

This means that there will be a precoding operation at the transmitter and decoding operation done at the receiver, both of them fulfilled at the subcarrier level. With the SVD, the channel matrix associated to the kth subcarrier is decomposed as

$$H(k) = U(k)\Lambda(k)V^H(k), \tag{3.4}$$

where $U(k)$ and $V^H(k)$ are the matrices used for the decoding and precoding processes, respectively. $\Lambda(k)$ = ($[\,\Lambda(k)_1 \;\; \Lambda(k)_2 \;\; \ldots \;\; \Lambda(k)_p]$ is a diagonal matrix composed by the P non-zero singular values of **H(k)**, with $\Lambda(k)_1 > \Lambda(k)_2 > \ldots > \Lambda(k)_p$. The precoded version of **S**(k) is **X**(k), where

$$X(k) = V(k)S(k), \tag{3.5}$$

with V(k) denoting the precoding matrix with dimensions T x P . The time-domain version of X(k) is obtained through an inverse discrete Fourier transform (IDFT), i.e.,

$$x^{(t)} = [x_1^{(t)}\; x_2^{(t)} \;\ldots\; x_{N_T}^{(t)}\,]. \tag{3.6}$$

After the precoding operation, the resulting signal is submitted to a nonlinear power amplifier (PA), and the output is

$$y^{(t)} = f(x^{(t)}). \tag{3.7}$$

The nonlinear PA is modeled as a bandpass memoryless nonlinearity, characterized by the amplitude modulation/amplitude modulation (AM/AM) and amplitude modulation/phase modulation (AM/PM) conversion functions A(.) and θ(.), respectively. For a given input $x_n^{(t)} = \left|x_n^{(t)}\right| \exp\left(jarg\left(x_n^{(t)}\right)\right)$, the PA yields

$$y_n^{(t)} = f\left(x_n^{(t)}\right) = A\left(\left|x_n^{(t)}\right|\right) \exp(j\left(\theta\left(x_n^{(t)}\right) + \arg\left(x_n^{(t)}\right)\right). \tag{3.8}$$

Without loss of generality, we considered the specific model of a solid state power amplifier (SSPA) [31]. This amplifier has negligible AM/PM characteristic and AM/AM characteristic given by

$$A\left(\left|x_n^{(t)}\right|\right) = \frac{\left|x_n^{(t)}\right|}{\sqrt[2q]{1+\frac{\left|x_n^{(t)}\right|^{2q}}{S_M}}}, \tag{3.9}$$

where S_M denotes the saturation level (naturally, the performance will be conditioned by the normalized saturation level S_M/σ_x, where σ_x is the variance of the real and imaginary parts of the precoded OFDM signal) and q defines the sharpness of the transition between the linear and nonlinear regions. When q =∞ the amplifier turns into an ideal envelope clipping with clipping level S_M .

Due to the Gaussian nature of the precoded OFDM signal at the nonlinear input, one can take advantage of the Bussgang's theorem [32]. This allows us to decompose a nonlinearly distorted Gaussian signal into two uncorrelated components: a useful component that is a scaled version of the input signal and a term that concentrates the nonlinear distortion [33]. Therefore, we may write the nonlinearly distorted signal at the output of the t^{th}PA as

$$y^{(t)} = f\left(x^{(t)}\right) = \alpha^{(t)} x^{(t)} + d^{(t)}, \tag{3.10}$$

where $d = \left[d_1^{(t)} \quad d_2^{(t)} \quad \dots \quad d_3^{(t)}\right]$ is the set of nonlinear distortion terms of the t^{th} branch and $\alpha^{(t)}$ is the scale factor associated to the t^{th} branch that can be obtained as

$$\alpha^{(t)} = \frac{E[x_n^{(t)} y_n^{*(t)}]}{E[|x_n^{(t)}|^2]} = \frac{E[x_n^{(t)} f^*(x_n^{(t)})]}{2\sigma_n^2}. \tag{3.11}$$

In fact, since it is assumed that the nonlinear characteristics of the power amplifiers are equal since the input power is considered the same, and the power of precoded signals is the same for all branches, the scale factor of (3.12) is independent of t and $\alpha^{(t)} = \alpha \, \forall \, t$. The discrete Fourier transform (DFT) of (3.10) yields the frequency-domain version of the signal to be transmitted $Y^{(t)} = DFT([y_1^{(t)} \; y_2^{(t)} \; \ldots \; y_{N_T}^{(t)}])$. Once again, from the Bussgang's theorem, we can separate into two uncorrelated components, leading to

$$Y^{(t)} = \alpha X^{(t)} + D^{(t)}, \tag{3.12}$$

where $D^{(t)} = DFT([d_1^{(t)} \; d_2^{(t)} \; \ldots \; d_{N_T}^{(t)}])$ represents the nonlinear distortion terms along the t^{th} branch. Under these conditions, the nonlinearly distorted signal for the kth subcarrier is

$$Y(t) = \alpha X(k) + D(k). \tag{3.13}$$

The nonlinearly amplified signals are transmitted through the frequency-selective channel represented in (3.1). Since the k^{th} channel is represented by **H**(k), the received signal is

$$W(k) = H(k)Y(k) + N(k), \tag{3.14}$$

where $N(k) = [N(k)_1 \quad N(k)_3 \; \ldots \; N(k)_R]^T$ represents the noise components associated to the k^{th} subcarrier. The power of the noise is $E = \left[|N(k)_r{}^2\right] = 2\sigma_N^2$, with σ_N^2 defined according to the desired SNR. Our SNR definition accounts for the impact of the nonlinear distortion effects and is dependent on the fraction of power wasted in the nonlinear distortion term. This "degradation" is measured by the ratio

$$\eta = \frac{P_u}{P_u + P_d} \, , \tag{3.15}$$

where $P_u = |\alpha|^2 \, E\left[\,\left|x_n^{(t)}\right|^2\right]$ and $P_d = E\left[\left|y_n^{(t)}\right|^2\right]$ - P_u represent the useful power and the power associated to the nonlinear distortion component, respectively.

Therefore,

$$SNR = \frac{E[|\alpha S(k)_r|^2]}{\eta E[|N(k)_r|^2]} = \frac{E[|\alpha S(k)_r|^2]}{2\sigma_N^2 \eta} \, . \tag{3.16}$$

By using (3.13) and (3.14), we have

$$W(k) = H(k)\big(\alpha X(k) + D(k)\big) + N(k). \quad (3.17)$$

To complete the SVD process, the received signal *W(k)* decoded by the matrix $U^H(k)$, leading to $R(k) = [R(k)_1 \ \ R(k)_2 \ \dots \ R(k)_p\ ]^T$. The decoded signal can be written as

$$\begin{aligned} R(k) &= U^H(k)W(k) = U^H(k)(H(k)Y(k) + N(k)) \\ &= U^H(U(k)\Lambda(k)V^H(k)\big(\alpha(k)X(k) + D(k)\big) + N(k) \\ &= \alpha\Lambda(k)S(k) + \Lambda(k)V^H(k)D(k) + U^H N(k). \quad (3.18) \end{aligned}$$

From (3.18), one can note that the SVD decomposition allows the transmission of P decoupled flat-fading OFDM streams that can be analyzed separately. The singular value k^{th} represents the flat-fading coefficient associated the pth stream of kth subcarrier.

3.1 Capacity of a linear SISO system

A linear SISO system is a system with only one transmitter antenna and a single receiver antenna, that as the addiction of AWGN to the signal. In Fig 3.1 it is shown the system.

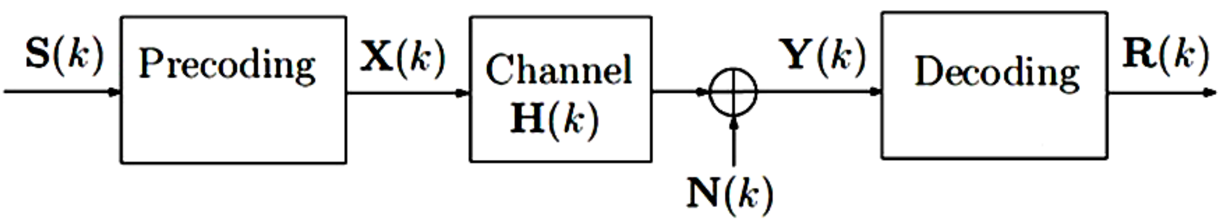

Fig 3.1 Linear SISO System

The signal S is submitted to a precoding operation that will result in the signal X, then it will be transmitted across the channel. When X reaches the receiver there is the addiction of AWGN represented in the fig 3.1 by N, that will result in the channel Y. After that, the signal will be submitted to the decoding operation, resulting finally in the signal R. The resulting capacity for such approximation can be directly taken from the Shannon theorem seen in (1.5).

In this case it is considered the use of a SVD technique as the precoding and decoding operation to deal with the effects of the channel. It is considered that there is a perfect channel estimation in both the receiver and transmitter, that will allow the use of the SDV technique on the channel, in order to deal with the effects that the channel will introduce to the signal. In Fig. 3.2 it is show the scheme for such a system.

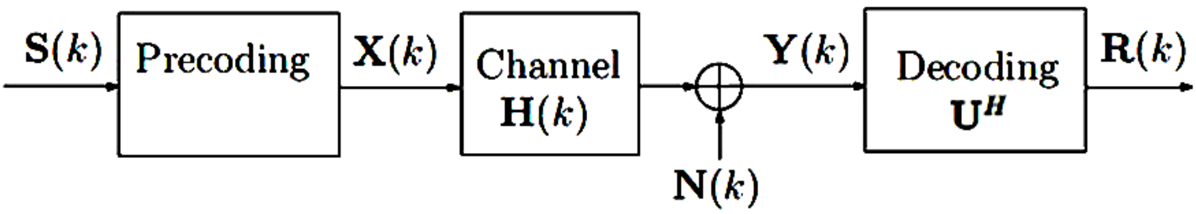

Fig 3.2 Linear SISO System with SVD

Considering a system with one transmitter antenna and one receiver antenna, ***H*** being the channel and the SVD decomposition of the channel being

$$H = U\lambda V^H, \qquad (3.19)$$

where V^H is the precoding matrix and U is the decoding matrix, the signal at the input of the channel is

$$X = VS. \qquad (3.20)$$

The received signal is

$$Y = HX + N = HVS + N$$

$$= U\lambda VV^H S + N = U\lambda S + N. \quad (3.21)$$

The decoding signal is obtained by multiplying (3.21) by U^H resulting in

$$R = U^H Y = U^H U\lambda S + U^H N$$

$$= \lambda S + U^H N = \lambda S + N'. \qquad (3.22)$$

In this case, the calculation of the capacity respects the Shannon theorem on capacity, allowing the easy calculation of the capacity of the channel.

Throughout the simulation of results, we proceeded to the calculation on the capacity of the SISO system using SVD. It was used the approximation equation

$$C = \log_2(1 + SNR). \qquad (3.23)$$

For this approximation, it is considered that the SNR can be described by

$$SNR = \frac{|\lambda|^2 E[|S|^2]}{E[|N'|^2]} . \qquad (3.24)$$

3.2 Capacity of a nonlinear SISO system

A nonlinear SISO system it is a system that has the addition of a nonlinear distortion added to the signal. It will be considered that the nonlinear effect can be compared to a Solid State Power Amplifiers, SSPA amplifier, since the multiplication for α and the addiction of interference can simulate the non linear effects to with the signal will be subjected. In fig 3.3 it is show the nonlinear SISO system.

In Fig. 3.3 it is possible to see the representation of the SISO system. S represents the symbol to be transmitted, X the result after the precoding, α is the scalar amplification of a SSPA, D is the distortion introduced by the SSPA, Y is the transmitted signal that will go through the channel H, N represents the AWGN, W is the signal before the decoding operation and R, the final received signal. Since we are considering a SISO system for a single symbol, all the factors are simple variables.

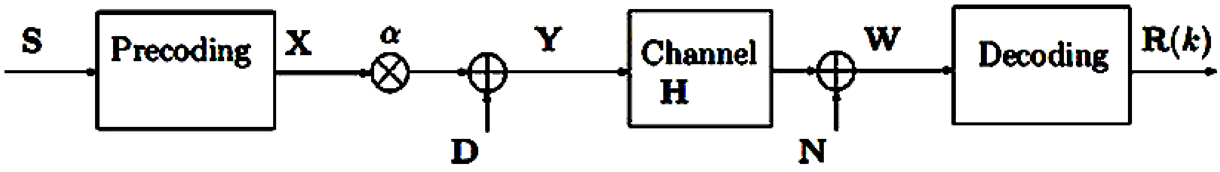

Fig 3.3 – Non Linear SISO system.

For a nonlinear SISO -OFDM transmission in ideal AWGN channels, the received signal for the k^{th} subcarrier is [16], [34]

$$Y(k) = \alpha S(k) + D(k) + N(k), \quad (3.25)$$

where S(k), D(k) and N(k) are the transmitted signal, the distortion signal and the noise signal for the k^{th} subcarrier. Therefore, the corresponding signal to interference and noise ratio (SINR) for the kth subcarrier is [35]

$$SINR^{SISO}(k) = \frac{|\alpha|^2 E[|S(k)|^2]}{E[|D(k)|^2] + E[|N(k)|^2]} \ . \quad (3.26)$$

In this case we considered the use of SSPA, to recreate the nonlinear effects that the signal is submitted. The nonlinearity can be viewed as the multiplication of the signal by a scalar α and the addiction of distortion represented in the figure as *D*.

So the system using a SVD precoding and decoding can be represented as seen in fig. 3.4.

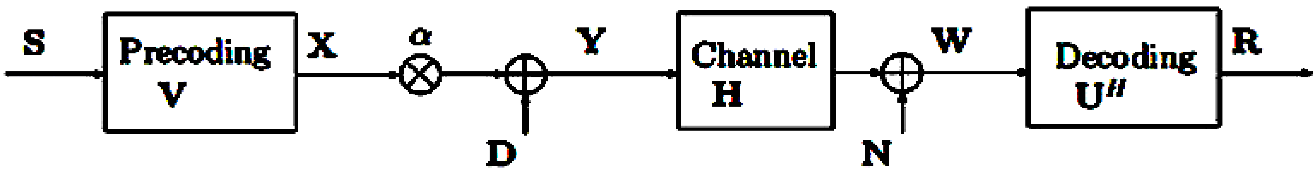

Fig 3.4 – Non Linear SISO system with SVD

With $\boldsymbol{H}$ being the channel and the SVD decomposition of the channel being

$$H = U\lambda V^H, \qquad (3.27)$$

V^H is the precoding matrix and U is the decoding matrix, the signal at the input of the channel is

$$X = VS. \qquad (3.28)$$

The signal after the nonlinear effect will be

$$Y = \alpha X + D. \qquad (3.29)$$

then, the resulting signal Y will be submitted to the channel H and will suffer the addiction of noise resulting in the received signal W:

$$\begin{aligned} W &= HY + N = \alpha HX + HD + N \\ &= \alpha HVS + HD + N = \alpha U\lambda V^H VS + U\lambda V^H D + N \\ &= \alpha U\lambda S + U\lambda V^H D + N. \qquad (3.30) \end{aligned}$$

The decoding signal is obtained by multiplying (3.29) by U^H resulting in

$$\begin{aligned} R &= U^H W = U^H \alpha U\lambda S + U^H U\lambda V^H D + U^H N \\ &= \alpha\lambda S + \lambda V^H D + U^H N = \alpha\lambda S + D' + N'. \qquad (3.31) \end{aligned}$$

Therefore, the corresponding signal to interference and noise ratio (SINR) for the kth subcarrier is (3.26)

For large SNR values, (i.e. $E[|N(k)|^2 \rightarrow 0$) the SINR reduces to the signal to interference ratio (SIR) and, for the k^{th} subcarrier, we may write

$$SIR^{SISO}(k) \simeq \frac{|\alpha|^2 E[|S(k)|^2]}{E[|D(k)|^2]}. \quad (3.32)$$

3.3 Capacity of a linear MIMO System

The analysis of the nonlinear MIMO system is in many ways equal do the approximations made to the linear SISO system. The channel will suffer the same decomposition but now we will be dealing with a large number of antennas, both in the receiver as in the transmitter.

The capacity associated to the k^{th}subcarrier of the p^{th} stream is

$$C^H(k)_p = \log_2(1 + SNR^H(k)_p)\,. \quad (3.33)$$

The total capacity associated to the k^{th}subcarrier is

$$C^H(k) = \sum_{p=1}^{P} C^H(k)_p. \quad (3.34)$$

And the average capacity of the block for a given channel realization is

$$C^{H'(k)} = \frac{1}{N}\sum_{k=1}^{N} C^H(k). \quad (3.35)$$

The fig 3.5 shows the evolution of the channel capacity associated to linear massive MIMO-OFDM systems considering frequency selective channels with L = 12, where G = 3, B = 4 and = 0.5. OFDM signals have N = 128 and M = 4. It can be observed in the figure that the capacity increases with the SNR. When the number of transmitter antennas is doubled, we can observe that the capacity also increases, the difference in capacity when it is observed T=8 and T= 16, it is not linear, as the SNR increases, the gain in capacity that is possible by duplicating the number of antennas, goes from around 5 bps/Hz in the case of SNR= -10dB's, up to around 20 bps/Hz in the case of SNR=30dB's. When we double the number of antennas from 16 to 32, the difference in capacity between T=32 and T= 16 goes from 6 bps/Hz in the case of SNR=-10dB's to 10 bps/Hz in the case of SNR=30dB's.

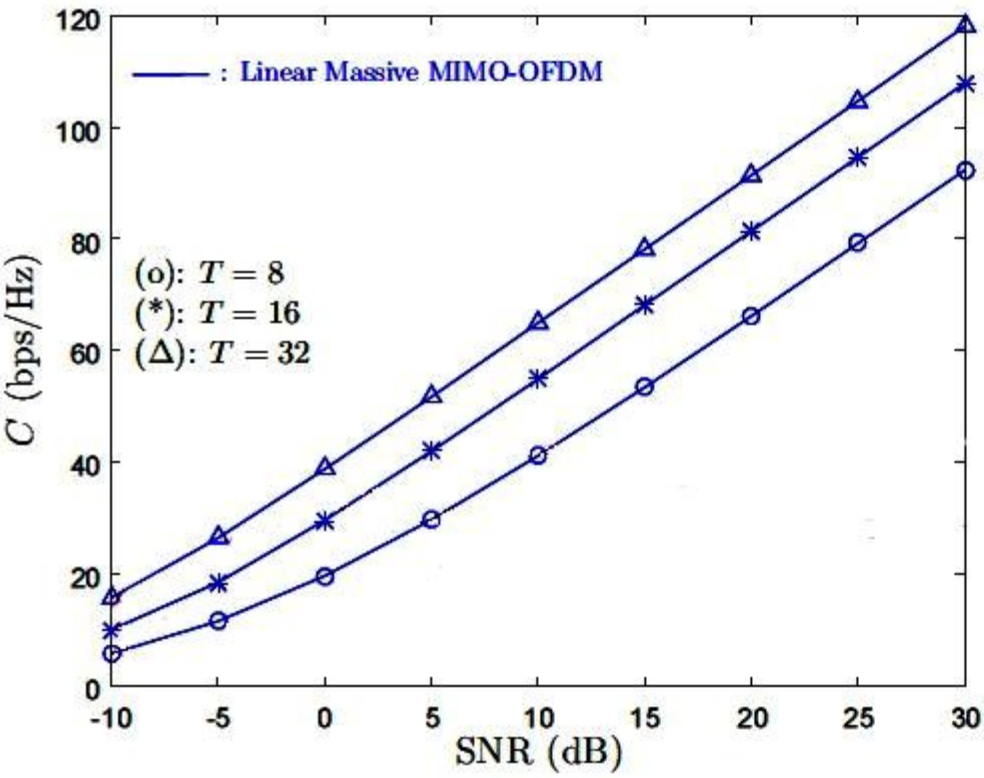

Fig 3.5- Evolution of capacity of the linear MIMO-OFDM for different values of T.

3.4 Capacity of a nonlinear MIMO System

The analysis of the nonlinear MIMO system is in many ways equal do the approximations made to the nonlinear SISO system. The channel will suffer the same decomposition, but now we will be dealing a large number of antennas, both in the receiver as in the transmitter. We start to obtain the SINR the k^{th}sub-carrier of the p^{th} stream considering a given channel realization. In order to do that, we write the received signal for the kth subcarrier of the p^{th} stream as (see (3.18))

$$R(k)_p = \alpha\Lambda(k)_p S(k)_p + \Lambda(k)_p D'(k)_p + N'(k)_p \,. \quad (3.36)$$

Being $\alpha\Lambda(k)_p S(k)_p$ the signal component and $\Lambda(k)_p D'(k)_p + N'(k)_p$ the noise and distortion component. Under these conditions, the SINR for the kth subcarrier of the p^{th}stream is

$$SINR^H(k)_p = \frac{|\alpha|^2|\Lambda(k)_p|^2 E[\left|S(k)_p\right|^2]}{|\Lambda(k)_p|^2 E\left[\left|D'(k)_p\right|^2\right] + E[|N'(k)_p|^2]}. \quad (3.37)$$

However, when T > R, it can be shown that [36][37]

$$E\left[\left|D'(k)_p\right|^2\right] = E[|\sum_{t=1}^{T} V^H(k)_{c,t}\, D(k)_t|^2]$$

$$\approx \frac{R}{T} E[|D(k)|^2]. \quad (3.38)$$

In fact, (3.37) reveals that there is a linear relation between the spectral distribution of the nonlinear distortion term in each one of the P streams and the nonlinear distortion term associated to a nonlinear SISO-OFDM system. This relation is approximately T/R, which shows that the robustness to nonlinear distortion effects increases with T (considering a fixed number of streams). Fig. 3.6 shows the spectral distribution of the nonlinear distortion term concerning the first stream (p=1) i.e. $E[|D'(k)_1|^2$ for R = 8 and different values of T as well as the spectral distribution of the nonlinear distortion term in a SISO-OFDM system.

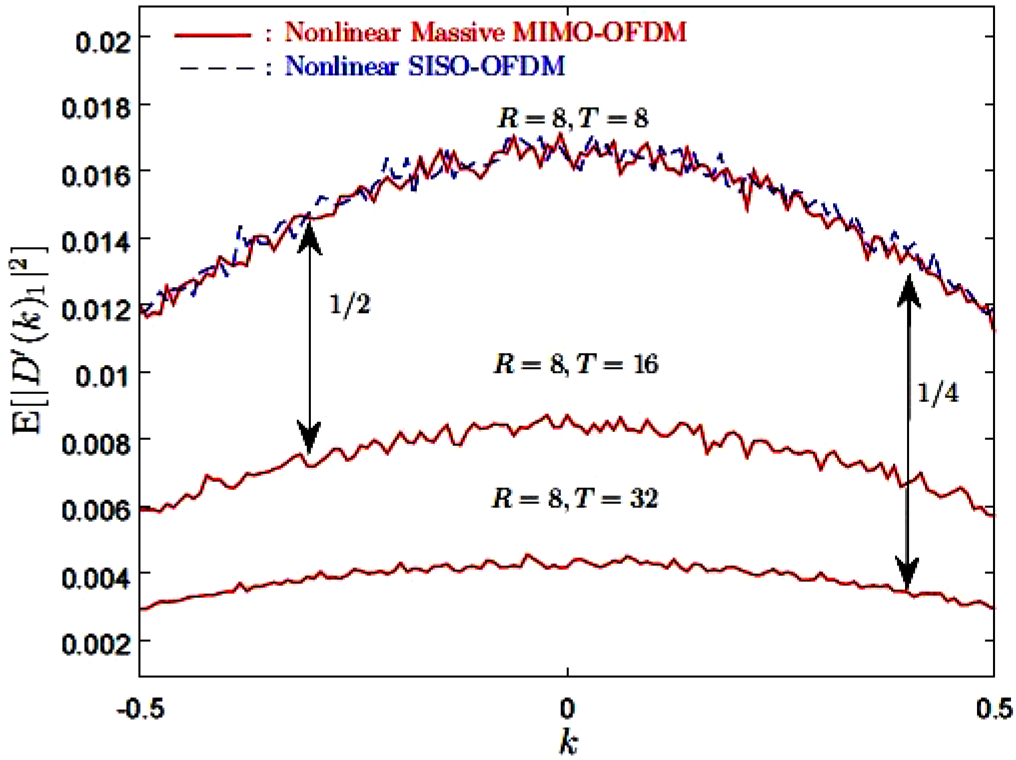

Fig 3.6 – Evolution of $E[|D(k)|^2]$ and $E[|D'(k)_1|^2]$ for different values of T and R=8.

The OFDM signals have N = 256 and M = 4 and the SSPA is parameterized by q = 1 and $\frac{S_M}{\sigma_x}$ = 0.5. From this figure it can be noted that for that the case of Nonlinear Massive MIMO with R = T = 8, it possible to have $E[|D'(k)_1|^2 \approx E[|D(k)|^2$, that meaning we have the same value of $E[|D(k)|^2]$ that is expected for the Nonlinear SISO -OFDM, T=R = 1 and in contrast, the spectral distribution of the nonlinear distortion term decreases by a factor of T/R = 1/2 when T = 16 and T/R = 1/4 when T = 32, which confirms that the distortion level can be greatly reduced when T≫ R. Therefore, (3.37) can be rewritten as

$$SINR^H(k)_p = \frac{|\alpha|^2 |\Lambda(k)_p|^2 E[|S(k)_p|^2]}{|\Lambda(k)_p|^2 \frac{R}{T} E\left[|D(k)_p|^2\right] + E[|N'(k)_p|^2]} . \quad (3.39)$$

The capacity associated to the k^{th}subcarrier of the p^{th} stream is

$$C^H(k)_p = \log_2(1 + SINR^H(k)_p)) \,. \quad (3.40)$$

The total capacity associated to the k^{th}subcarrier is

$$C^H(k) = \sum_{p=1}^{P} C^H(k)_p, \quad (3.41)$$

and the average capacity of the block for a given channel realization is

$$C^{H\prime}(k) = \frac{1}{N} \sum_{k=1}^{N} C^H(k). \quad (3.42)$$

Therefore, the total capacity can be obtained by averaging (3.42) over the channel realizations (i.e. over *H*),

$$C = E_H[C^{H\prime}] \,. \; (3.43)$$

Fig. 3.7 shows the evolution of the channel capacity associated to nonlinear massive MIMO-OFDM systems considering frequency selective channels with L = 12, where G = 3, B = 4 and $\frac{s_M}{\sigma_x}$= 0.5. OFDM signals have N = 128 and M = 4. We considered massive MIMO-OFDM systems with R = 8 and different values of T. The SSPA is parameterized by s_m= x = 0.5 and q = 1.

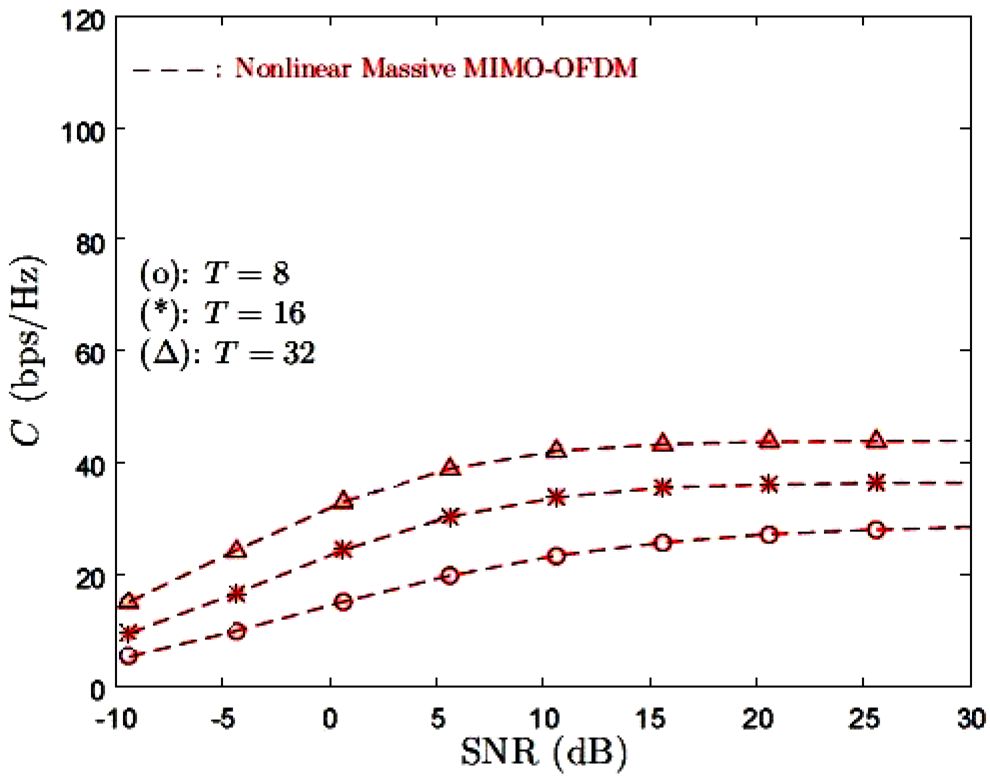

Fig. 3.7 - Evolution of the capacity for nonlinear channel for $\frac{s_M}{\sigma_x} = 0{,}5$, q = 1, R = 8 and different values of T.

From figure 3.7 it can be noted that as the number of transmit antennas increases, not only the linear channel capacity increases (as expected), but also the capacity associated to the nonlinear massive MIMO-OFDM increases. In fact, the "floor level" of the nonlinear channel capacity increases due to the fact that the PSD associated to the nonlinear distortion term decreases with T for a fixed number of streams. For low SNR, it should be pointed out that the linear and nonlinear channel capacities are not exactly equal. The difference between them is related with the fraction of power wasted in the nonlinear distortion component (see (3.15)).

Fig. 3.8 shows the evolution of η considering different saturation levels and different values of q. As expected, the stronger the nonlinearity the larger the degradation, since the distortion component is higher (moreover, there is more power wasted in its transmission, i.e., decreases). Meaning that to counterbalance this effect, with will need to use more power in the signal transmission, in order to increase the SINR. When an ideal envelope clipping is considered (i.e., for q=+∞), the degradation with S_M/σ_x= 0.5 can be 0.5 dB.

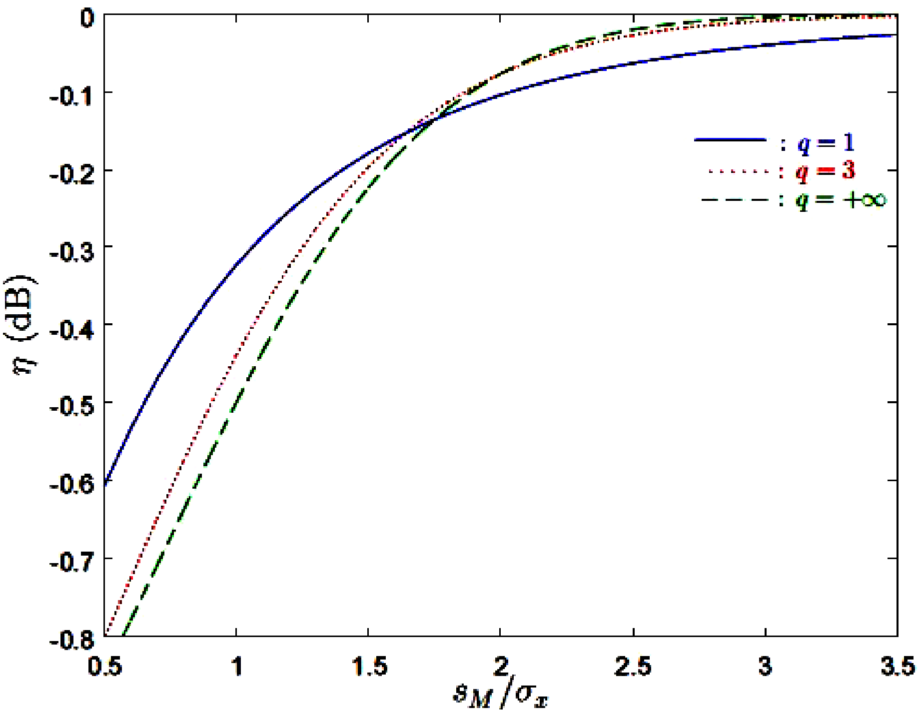

Fig. 3.8. Evolution of the degradation for an SSPA with different saturation levels and different values of q.

Fig. 3.9 shows the evolution of the linear and nonlinear channel capacities for R = 8 and T = 32 considering an SSPA with q = 1 and different saturation levels. From the figure it can be noted that the larger the saturation level, the better the capacity. In fact, the capacity floors increase substantially with S_M/σ_x. [38]

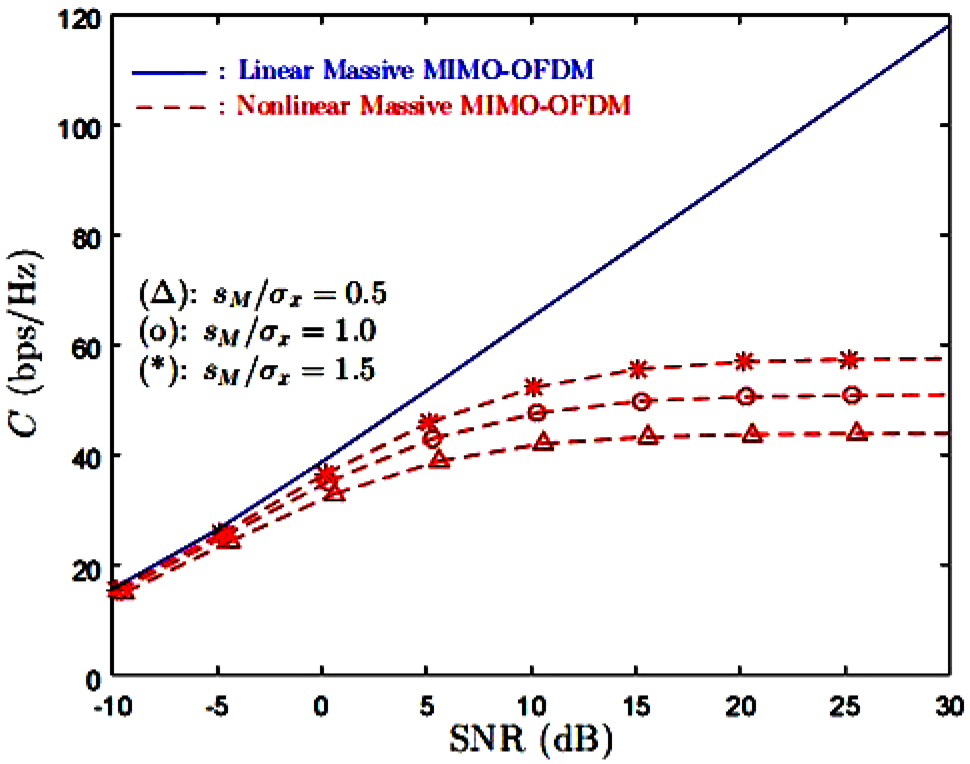

Fig 3.9- Evolution of the channel capacity for R = 8, T = 32, different saturation levels and q = 1.

It is possible to determine that for different saturation levels the capacity of the massive MIMO system also changes. With the increase of $\frac{S_M}{\sigma_x}$ the capacity of the system also increases, and for the considered SNR interval the difference can be as high as 7 bps/Hz for SNR=30dB's and 20dB's.

By analysis of the several simulations it can be show that the evolution of capacity does not have a linear behavior in terms of gain of bps/Hz. But it can be clarified that as expected the bigger the number of transmission antennas, the higher it will be the capacity, and that there is an increase of the capacity according to the $\frac{S_M}{\sigma_x}$ relation.

4

Conclusion

In this thesis it was studied the capacity of a MIMO-OFDM system in the case of linear and nonlinear case. It was presented an analytical method for obtaining the capacity conditioned to a given channel realization, using the SVD technique. As expected, the capacity increases with the number of transmit antennas in both cases of linear and nonlinear effects. It was shown that the capacity decreases as we increase the nonlinear distortion effects. However, for a fixed number of independent data streams, this capacity degradation can be compensated by increasing the number of antennas at the transmitter side.

Given the work finished in this thesis, there are still a lot of opportunities for future research on massive MIMO-OFDM that related to this thesis. We list below several topics that might be interesting:

The analysis of the capacity of a massive MIMO-OFDM with Matched filter technique.

The analysis of the capacity of a massive MIMO-OFDM with Zero Forcing technique.

References

[1] D. Tse and P. Viswanath, Fundamentals of wireless communication, Cambridge, MA: Cambridge University Press, 2005.

[2] A. C Brooks and S. J, Hoelzer, "Design and Simulation of Orthogonal Frequency Division Multiplexing signaling", Department of Electrical Engineering, Bradley University, Peoria, IL, Project Report, May, 2001.

[3] S. J. Vaughan-Nichols (2001, November 14), OFDM: Old Technology for New Market, Tutorial article [Online], Wi-FI Planet. Available: ttp://www.wifi-planet.com/tutorials/article.php/1500641/OFDM-Old-Technology-for-New-Markets.htm.

[4] R. V. Nee, OFDM for Wireless Multimedia Communications, Boston, MA: Artech House Publishers, 1999.

[5] A. Doufexi, S. Armour, M. Butler, A. Nix, D. Ull, J. McGeehan and P.Karlsson, "A Comparison of the HIPERLAN/2 and IEEE 802.11a Wireless Standards", IEEE Communications Magazine, vol. 40, pp. 172-180, 2002.

[6] A. Katalinic, R. Nagy and, R. Zentnerl, "Benefits of MIMO Systems in Practice: Increased Capacity, Reliability and Spectrum Efficiency" in 48 th International Symposium ELMAR, Zadar, Croatia, June 2006.

[7] B. Sklar, Digital Communications: Fundamentals and Applications,2 nd edition, Upple Saddle River, NJ: Prentice Hall, 2001.

[8] B. Sklar, "Rayleigh Fading Channels in Mobile Digital Communication Systems Part I: Characterization". IEEE Communications Magazine, vol. 35, pp. 90–100, 1997.

[9] A. B. do Paula, "An Introduction to Doppler effect and fading in mobile Communications", Master's thesis, Report Number A679062, Naval Postgraduate School, Montreal, CA, 1992.

[10] J. G. Proakis,, Digital Communications, New York, NY: McGraw-Hill Book Company, 1989.

[11] C. Oestges and B. Clerckx, MIMO Wireless Communications: From Real-world Propagation to Space-time Code Design, San Diego, CA: Academic Press, 2007.

[12] M. K. Simon and M. S. Alouini, Digital Communication Over Fading Channels, 2 nd Edition, Hoboken, NJ: Wiley-IEEE Press, 2004.

[13] F. Boccardi, R. Heath, A. Lozano, T. Marzetta, P. Popovski, "Five disruptive technology directions for 5G", IEEE Communications Magazine, Vol. 52, No. 2, pp.74-80, Feb. 2014.

[14] F. Rusek, D. Persson, B. K. Lau, E. G. Larsson, O. Edfors, F. Tufvesson, and T. L. Marzetta, "Scaling up MIMO: opportunities and challenges with very large arrays", IEEE Signal Processessing Magazine, Vol. 30, No. 1, pp. 40-60, Jan. 2013.

[15] Hien Quoc Ngo, "Massive MIMO: Fundamentals and System Designs", Linköping University Electronic Press, pp. 19-20 Jan 16, 2015

[16] P. Banelli and S. Cacopardi, "Theoretical analysis and performance of OFDM signals in nonlinear AWGN channels," IEEE Trans. Commun., ol. 48, no. 3, pp. 430–441, Mar. 2000.

[17] K. Baum, B. Classon and P. Sartori, Principles of Broadband OFDM Cellular System Design, Hoboken, NJ: John Willey & Sons, 2010.

[18] X. Li and F. Ng , "Using cyclic prefix to Mitigate Carrier Frequency and Timing Asynchronism in Cooperative OFDM Transmissions" in ACSSC '06, Fortieth Asilomar Conference on Signals, Systems and Computers, 2006.

[19] S. Wang, C. Li, “A low-complexity PAPR reduction scheme for SFBC MIMO-OFDM systems,” IEEE Signal Process. Lett., vol. 50, no. 1, pp. 89–101, Jan. 2002.

[20] Y. Rahmatallah and S. Mohan, “Peak-to-average power ratio reduction in OFDM systems: a survey and taxonomy,” IEEE Commun. Surveys Tuts., vol. 15, no. 4, pp. 1567–1592, Mar. 2013.

[21] X. Li and L. Cimini Jr., “Effects of clipping and filtering on the performance of OFDM,” IEEE Commun. Lett., vol. 2, no. 5, May 1998.

[22] H. Ochiai and H. Imai, “Performance analysis of deliberately clipped OFDM signals,” IEEE Trans. Commun., vol. 50, no. 1, pp. 89–101, Jan. 2002.

[23] L. Zheng and D. N. C. Tse , “Diversity and Multiplexing: A Fundamental Tradeoff in Multiple-Antenna Channels”, IEEE Transactions on Information Theory, vol. 49, pp. 1073-1096, 2004.

[24] R. Heath, Jr. and A. Paulraj, “Switching between multiplexing and diversity based on constellation distance” in Proc. Allerton Conf. Communication, Control and Computing, Monticello, IL, 2000.

[25] D.Agrawal, V Tarokh, A Naguib and N Seshadri,, Space time coded OFDM for highdata rate wireless communication over wide band channels in Proc of 48 Th IEEE Vehicular technology Conference, vol.3, pp. 2232—2236, Ottawa, Canada, 1998.

[26] Y S. Cho, J. Kim, W. Y. Yang and C.G. Kang, MIMO-OFDM Wireless Communications with MatLab, Hoboken, NJ: Wiley Press, 2010.

[27] S. M. Alamouti, “A simple transmit diversity technique for wireless

communications”, IEEE journal on select areas in communications ,vol. 16, pp. 1451-1458, 2008.

[28] T. M. Duman and A. Ghrayeb, Coding for MIMO Communication Systems, Hoboken: NJ: Wiley Press, 2008.

[29] Y. Li, "Simplified channel estimation for OFDM systems with multiple transmit antennas," IEEE Trans. Wireless Commun., vol. 1, no. 1, pp. 67–75, Jan. 2002.

[30] G. Lebrun, J. Gao, M. Faulkner, "MIMO transmission over a timevarying channel using SVD," IEEE Trans. Wireless Commun., vol. 4, no. 2, pp. 757–764, Mar. 2005.

[31] G. Santella and F. Mazzenga, "A model for performance evaluation in M-QAM-OFDM schemes in presence of nonlinear distortions", IEEE VTC'1995, Chicago, USA, July 1995.

[32] J. J. Bussgang, "Crosscorrelation functions of amplitude-distorted gaussian signals," M.I.T. RLE Technical Report, no. 216, pp. 1–14, Mar. 1952.

[33] H. Rowe, "Memoryless nonlinearities with gaussian input: elementary results," Bell System Tech. Journal, vol. 61, no. 67, pp. 1519–1526, Sept. 1982.

[34] R. Dinis and A. Gusm˜ ao, "A Class of nonlinear signal processing schemes for bandwidth-efficient OFDM transmission with low envelope fluctuation," IEEE Trans. Commun., vol. 52, no. 11, pp. 2009–2018, Nov. 2004.

[35] H. Ochiai and H. Imai, "Performance analysis of deliberately clipped OFDM signals," IEEE Trans. Commun., vol. 50, no. 1, pp. 89–101, Jan. 2002.

[36] I. Iofedov and D. Wulich, "MIMOOFDM With Nonlinear Power Amplifiers," IEEE Trans. Commun., vol. 63, no. 12, pp. 4894–4904, Out. 2015.

[37] J. Guerreiro, R. Dinis and P. Montezuma, "On the assessment of nonlinear distortion effects in MIMO-OFDM systems", IEEE VTC'16 (Spring), Nanjing, China, May 2016.

[38] P. Fernandes, J. Guerreiro, R. Dinis and P. Montezuma, " On the Capacity of Nonlinear Massive MIMO-OFDM Systems ", In Proc. of IEEE VTC'16 (Fall), Montreal, Canada, Sept. 2016